

## Article

# Development of a Novel Double-Sulfate Composite Early Strength Agent to Improve the Hydration Hardening Properties of Portland Cement Paste

Yuli Wang , Luyi Sun, Songhui Liu \* , Shuaijie Li, Xuemao Guan and Shuqiong Luo

Henan Key Laboratory of Materials on Deep-Earth Engineering, School of Materials Science and Engineering, Henan Polytechnic University, Jiaozuo 454003, China

\* Correspondence: liusonghui@hpu.edu.cn

**Abstract:** A novel double-sulfate composite early strength agent (DSA) incorporating aluminum sulfate and sodium sulfate was developed to improve the early strength of Portland cement paste. The effect of the DSA dosage on the setting and hardening properties, hydration process, hydration product composition, microstructure, and pore structure of the Portland cement paste was investigated to reveal its synergistic enhancement mechanism. The results show that the 3 d and 28 d compressive strengths of the Portland cement paste incorporating with 1.0% aluminum sulfate and 1.5% sodium sulfate performed the best, with a 21.3% and 29.7% increase, respectively, compared to the control group. The heat of hydration, XRD, TG, SEM, and MIP tests showed that aluminum sulfate and sodium sulfate acted synergistically, with more AFt (Ettringite) being produced by the synergistic use of 1.0% aluminum sulfate and 1.5% sodium sulfate. Moreover, the hydration of  $C_3S$  and  $C_2S$  was accelerated, which resulted in a denser microstructure.

**Keywords:** Portland cement; aluminum sulfate; sodium sulfate; hydration; synergistic enhancement mechanism



**Citation:** Wang, Y.; Sun, L.; Liu, S.; Li, S.; Guan, X.; Luo, S. Development of a Novel Double-Sulfate Composite Early Strength Agent to Improve the Hydration Hardening Properties of Portland Cement Paste. *Coatings* **2022**, *12*, 1485. <https://doi.org/10.3390/coatings12101485>

Academic Editor: Paolo Castaldo

Received: 12 September 2022

Accepted: 3 October 2022

Published: 6 October 2022

**Publisher's Note:** MDPI stays neutral with regard to jurisdictional claims in published maps and institutional affiliations.



**Copyright:** © 2022 by the authors. Licensee MDPI, Basel, Switzerland. This article is an open access article distributed under the terms and conditions of the Creative Commons Attribution (CC BY) license (<https://creativecommons.org/licenses/by/4.0/>).

## 1. Introduction

Nowadays, silicate cement, also known as Portland cement, is an indispensable material for the construction industry. With the continuous development of society and the continuous innovation of infrastructure today, the demand for cement is huge. Yet, to satisfy specific requirements and save time, admixtures are generally required to increase the early strength of Portland cement [1–5]. For example, Portland cement with water-reducing and early-strengthening agents is often used when carrying out the projects for precast elements, construction of paving, grouting, and filling [6], which can significantly speed up the process of the project. At present, there are three main types of early strength agents being used: organic salts, inorganic salts, and compounds [7,8]. In addition, some special materials can also improve the strength of cement paste [9–12]. Of these, inorganic salts are widely used as their effect on Portland cement is often immediate and obvious [13]. However, the use of an early-strengthening agent containing only one inorganic salt for cement has certain limitations (for example, the use of aluminum sulfate alone does not result in a cement that exhibits higher early strength) [14–16], so the study of composite early-strengthening agents that can better improve the performance of cement is the primary trend of current research [3,17].

Aluminum sulfate is widely used as an alkali-free early strengthener with low contamination and good stability, and it improves worker safety [18,19]. Research shows that aluminum sulfate added to cement promotes hydration and hardening [3,20–22]. Chen C et al. [22] supported that aluminum sulfate dissociates aluminum ions and sulfate ions in the cement paste, which will combine with calcium and hydroxide ions in the cement to form AFt (Ettringite). The exothermic generation of AFt from the above reactions

promotes the hydration of  $C_3A$  and the production of more AFt, resulting in reduced flow and setting time of the cement paste. Guosheng Ren et al. [21] found that the addition of aluminum sulfate resulted in the rapid generation of AFt during the initial reaction period and advanced the hydration of  $C_3S$ . The high-valent metal ion  $Al^{3+}$  can squeeze the diffusion bilayer of C–S–H gels, which promotes the agglomeration of C–S–H gels [3]. The early strength agent studied by Yang Renhe et al. [20] can make cement paste set and strengthen early, the main component of this early strength agent is aluminum sulfate.

The use of sodium sulfate early strengthening agents to modify cement properties has also been studied [2,13,23–26]. It has been found that when sodium sulfate is added to cement, the introduced sulfate and the calcium ions in the cement will participate in the hydration of  $C_3A$  and promote the production of AFt [23,27]. The combination of sodium and hydroxide ions leads to an increase in the alkalinity of Portland cement paste, which increases the solubility of  $C_3A$  and calcium sulfate and promotes the hydration of  $C_3S$  [2,13]. However, the soluble salts formed by the sodium ions can dissolve and precipitate, causing swelling and cracking of the cement [13,28].

In conclusion, the use of a certain amount of aluminum sulfate or sodium sulfate alone will result in cement exhibiting higher early strengths. However, it is less clear whether the synergistic use of sodium sulfate and aluminum sulfate will result in cement with more desirable early strength and compensate for the later strength reversal caused by the addition of sodium sulfate. In addition, the doping ratios for synergistic use and the mechanism of action during synergistic use have not been well understood.

To address these issues, this work investigated the effect of different ratios of aluminum sulfate and sodium sulfate on the performance of the cement and investigated the appropriate synergistic balance to achieve a better early strength of the cement, as well as an excellent overall performance. The synergistic mechanism of aluminum sulfate and sodium sulfate on the hydration and hardening of the cement was also investigated by the heat of hydration, XRD, TG, SEM, and MIP.

## 2. Experimental Materials and Experimental Protocol

### 2.1. Experimental Materials

In this experiment, the Ordinary Portland cement (OPC) of PO·42.5 was used, the properties of which meet the standard Chinese GB175-2007 [29], the specific composition and properties of this cement are shown in Tables 1–3 below. Aluminum sulfate ( $Al_2(SO_4)_3 \cdot 18H_2O$ ) and anhydrous sodium sulfate ( $Na_2SO_4$ ) are chemically pure reagents, and the purity is more significant than 99.0%. The water used is laboratory tap water.

**Table 1.** The physical properties of the Portland cement.

Fineness/%	SSA ( $m^2/kg$ )	Stability	Setting Time /Min		Flexural Strength/MPa		Compressive /MPa	
			Initial	Final	3 d	28 d	3 d	28 d
0.8	366	qualified	200	250	6.0	9.5	30.1	50.5

**Table 2.** The chemical composition (wt%) of the Portland cement.

CaO	SiO <sub>2</sub>	Al <sub>2</sub> O <sub>3</sub>	Fe <sub>2</sub> O <sub>3</sub>	MgO	SO <sub>3</sub>	Na <sub>2</sub> O	K <sub>2</sub> O	Loss
61.86	23.17	5.37	3.32	2.78	2.36	0.36	0.20	0.13

**Table 3.** The mineral composition (wt%) of the Portland cement.

C <sub>3</sub> S	C <sub>2</sub> S	C <sub>3</sub> A	C <sub>4</sub> AF	Gypsum	Calcite	Amorphous
58.68	15.03	9.34	7.80	2.65	3.62	2.88

## 2.2. Experimental Protocol

### 2.2.1. Design Ratios

Table 4 lists the design groups of this experiment. The water to cement ratio in this experiment was 0.4, and the chemical admixture was sieved through 200 mesh and used.

**Table 4.** Design ratio.

Groups	Al <sub>2</sub> (SO <sub>4</sub> ) <sub>3</sub> ·18H <sub>2</sub> O <sup>1</sup> /%	Na <sub>2</sub> SO <sub>4</sub> <sup>1</sup> /%	Cement/g	Water/g
Control	-	-	500	200
Al0.5%	0.5	-	500	200
Al1.0%	1.0	-	500	200
Al1.5%	1.5	-	500	200
Al2.0%	2.0	-	500	200
Na0.5%	-	0.5	500	200
Na1.0%	-	1.0	500	200
Na1.5%	-	1.5	500	200
Na2.2%	-	2.0	500	200
Al1.0% + Na0.5%	1.0	0.5	500	200
Al1.0% + Na1.0%	1.0	1.0	500	200
Al1.0% + Na1.5%	1.0	1.5	500	200
Al1.05 + Na2.0%	1.0	2.0	500	200

<sup>1</sup> mixed in as a percentage by mass of cement.

### 2.2.2. Preparation of Portland Cement Paste

The prepared aluminum sulfate and sodium sulfate was ground to a powder and then mixed with cement and stirred well. According to the General “Portland Cement” National Standard (GB175-2007) [29], it takes 15 s to add the mixed cement and water to the mixing pot, then stirs for 2 min at low speed, then shakes and finally stir for 2 min at high speed.

### 2.2.3. Test for Setting Time

The Vicar method was used to test the setting time according to the “Test Method for the Standard Consistency, Setting Time and Settlement of Cement” (GB/T1346-2011) [30]. The setting time was tested separately three times to obtain the average.

### 2.2.4. Test for Compressive Strength

The prepared paste was molded in a clean 40 × 40 × 40 mm mold and covered with cling film to prevent water evaporation, then placed in a standard curing room for one day, after which de-molded and continue curing was conducted. The standard curing room temperature was 20 ± 2 °C and the humidity was ≥95%, in line with the curing conditions.

According to the “Standard for Mechanical Properties of Plain Concrete Test Methods” (GB50081-2019) [31], compressive strength tests were carried out on 3 d and 28 d specimens, with each group of specimens measured three times and the average value taken.

### 2.2.5. Hydration Heat Release

The hydration heat of Portland cement with different admixtures was carried by using an isothermal conductivity calorimeter (ICC, TAM Air, Newcastle, DE, USA). A sample of 2.5 g of cement mixture according to Table 4 was blended into the calorimetric apparatus and equilibrated for two hours to exclude heat flow errors after installation. For each group, the mixture test at 20 °C.

### 2.2.6. XRD Analysis

The specimens that had been soaked in anhydrous ethanol for 24 h were dried in a vacuum oven at 60 °C, then ground into a powder and sieved through 200 mesh. A Smart lab X-ray diffractometer (CuKα radiation, λ = 1.54056 Å, Rigaku Smart Lab, Tokyo, Japan) at a scan rate of 10 °C/min and an angle of 5–80° was used for the XRD analysis.

### 2.2.7. TGA Analysis

The TGA tests were started on the dried and ground powder using an HCT-3 micro-computer differential thermal equilibrium (Rigaku, Tokyo, Japan) with a carry temperature of 40–900 °C and a ramp-up rate of 10 °C per minute. Samples from each group of cement, after curing for 3 days and 28 days, were used for testing. After curing, the main composition of the medium (AFt, Ca(OH)<sub>2</sub> and CaCO<sub>3</sub>) in the cement paste was analyzed. According to the study, the mass percentage of AFt produced ( $m_{AFt}$ ) was calculated based on the weight loss from dehydration of AFt at 50–150 °C (ignoring the loss of other components bound to water). The mass percentage of calcium hydroxide produced ( $m_{CH}$ ) was calculated from the weight loss when CH was dehydrated at 400–500 °C and CaCO<sub>3</sub> was decomposed at 550–900 °C [32,33]. The following are the relevant chemical reactions.



The following are the content calculations.

$$m_{AFt}(\%) = m_{\text{H}_2\text{O}} \times \frac{M_{AFt}}{32M_H} \quad (4)$$

$$m_{CH}(\%) = m_H \times \frac{M_{CH}}{M_H} + m_{CC} \times \frac{M_{CC}}{M_{\text{CO}_2}} \quad (5)$$

where,  $m_{AFt}$  is the mass fraction percentage of AFt produced,  $m_{\text{H}_2\text{O}}$  is the mass fraction percentage of water loss from crystallization lost by thermal decomposition of the thermal decomposition of AFt,  $M_{AFt}$  is the molar mass fraction of AFt,  $m_H$  is the mass fraction percentage of water loss by decomposition of CH,  $m_{CC}$  is the mass fraction percentage of weight loss by decomposition of CaCO<sub>3</sub>,  $M_H$  indicates the molar mass of H<sub>2</sub>O,  $M_{CC}$  is the molar mass of CaCO<sub>3</sub> and  $M_{\text{CO}_2}$  is the molar mass of CO<sub>2</sub>.

### 2.2.8. SEM Analysis

According to the sample-making requirements, the middle part of the specimen was taken separately and sealed in anhydrous ethanol for 24 h to terminate the hydration. Before starting the SEM experiment, the samples were dried in a vacuum oven at 40 °C for a further 24 h, then the samples were treated for electrical conductivity and tested with a Merlin Compact SEM scanner (Carl Zeiss NTS GmbH, Oberkohan, Germany).

### 2.2.9. MIP Analysis

The specimens with ages of 28 d were cut to samples of 10 mm in height and width and 15 mm in length, then they were sealed in anhydrous ethanol for 24 h to terminate hydration, and then put into a vacuum drying oven to dry at 40 °C for 24 h. The porosity and pore size distribution of the samples was tested by using the Automatic Pores IV 9500 Mercury Porosimeter (Micromeritics, Atlanta, GA, USA).

## 3. Results and Discussion

### 3.1. Effect of the DSA on the Setting Time of Portland Cement Paste

The effect of the DSA on the setting time of Portland cement paste is shown in Figure 1. It shows that the initial setting time and final setting time decreased continuously with the increase of aluminum sulfate dosing. Compared to the control group, for each increase of 0.5% aluminum sulfate, the initial setting time decreased by 24.0%, 31.6%, 41.3%, 47.4%, and the final setting time decreased by 19.6%, 26.4%, 28.4%, 35.2%, respectively. The effect of sodium sulfate on the initial and final setting times of Portland cement paste was less pronounced than that of aluminum sulfate; the initial and final setting times

of Portland cement paste fluctuated upwards and downwards as the amount of sodium sulfate was increased. Compared to the control group, for each increase of 0.5% sodium sulfate, the initial setting time of the cement was reduced by  $-4.6\%$ ,  $3.6\%$ ,  $9.2\%$ ,  $5.6\%$ , and the final setting time by  $4.4\%$ ,  $-2.4\%$ ,  $0.8\%$ ,  $8.4\%$ , respectively. When the DSAs were used in combination, the initial and final setting times of the cement were insignificant when the amount of sodium sulfate was increased by 0.5% and using 1.0% aluminum sulfate as a quantification. Compared to the control group, the initial setting time was reduced by  $37.2\%$ ,  $38.3\%$ ,  $30.1\%$ ,  $28.6\%$ , and the final setting time was reduced by  $26.8\%$ ,  $16.0\%$ ,  $24.4\%$ ,  $24.0\%$ , respectively, while compared to the Al1.0% group, the initial setting time was reduced by  $8.21\%$ ,  $9.70\%$ ,  $-2.24\%$ ,  $-4.48\%$ , and the final setting time was reduced by  $0.54\%$ ,  $-14.13\%$ ,  $-2.72\%$ ,  $-3.26\%$ , respectively. In summary, the setting time of the Portland cement paste decreases as the aluminum sulfate dose increases; in contrast, the effect of sodium sulfate on the setting time of the Portland cement paste is not significant. When aluminum sulfate and sodium sulfate were used in combination, it was the aluminum sulfate that had the main effect on the setting time of the Portland cement paste.

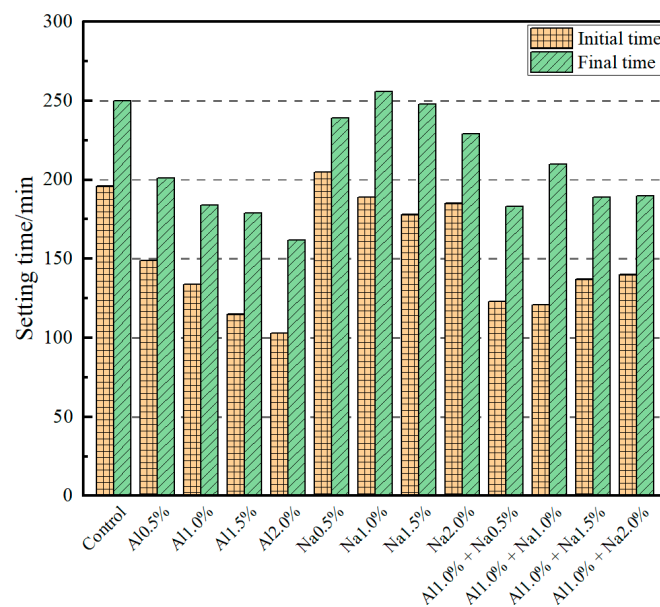


**Figure 1.** Effect of different amounts of the DSA on setting time of Portland cement paste.

### 3.2. Effect of the DSA on the Compressive Strength of Portland Cement Paste

The compressive strengths of the Portland cement paste at 3 d and 28 d for different doses of the DSA are shown in Figure 2. It was observed that the compressive strength of Portland cement paste at 3 d and 28 d increased first and then decreased with increasing admixture levels, whether aluminum sulfate or sodium sulfate was used alone or in combination with aluminum sulfate and sodium sulfate. Compared to the control group, for each 0.5% increase in aluminum sulfate, the compressive strength of Portland cement paste at 3 d was enhanced by  $1.8\%$ ,  $7.2\%$ ,  $6.0\%$ ,  $4.8\%$ , and the compressive strength at 28 d by  $7.9\%$ ,  $22.4\%$ ,  $19.4\%$ ,  $-4.4\%$ , respectively. The best early strength was achieved at 1.0% of aluminum sulfate and no inversion of strength occurred at a later stage. Compared to the control group, for each 0.5% increase in sodium sulfate, the compressive strength of Portland cement paste at 3 d was increased by  $9.6\%$ ,  $10.2\%$ ,  $10.5\%$ ,  $0.0\%$ , and the compressive strength at 28 d was increased by  $6.7\%$ ,  $7.9\%$ ,  $20.6\%$ ,  $-14.9\%$  for each 0.5% increase in sodium sulfate. Although the compressive strengths of the Na1.0% and Na1.5% groups at 3 d were almost the same, the compressive strength of the Na1.5% group at 28 d was much greater than that of the Na1.0% group, so the 1.5% sodium sulfate admixture had the best effect in improving the compressive strength of the cement. The results show that 1.0% aluminum sulfate and 1.5% sodium sulfate have the greatest influence on the

compressive strength of Portland cement paste, the strength at 3 d was enhanced by 13.2% and 10.1% over the Al1.0% and Na1.5% groups, respectively, and the strength at 28 d was enhanced by 29.7%, 5.9% and 7.5% over the control, Al1.0%, and Na1.5% groups, respectively, with no decrease in compressive strength compared to the blank group.

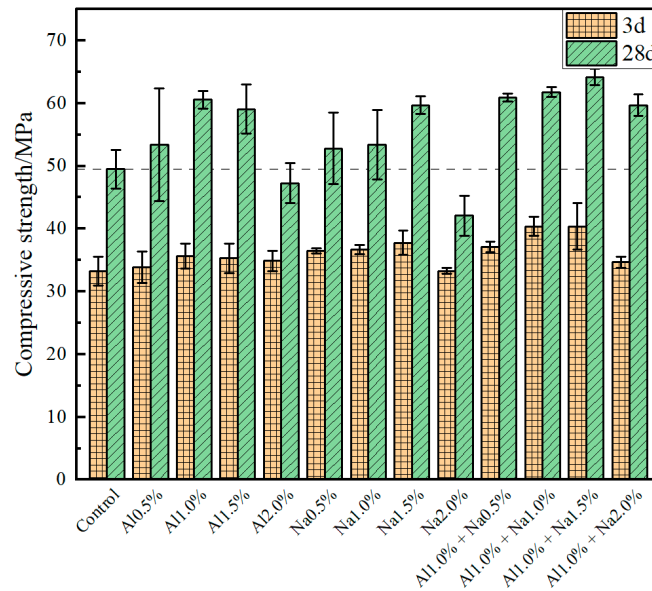


Figure 2. Effect of different amounts of the DSA on compressive strength of Portland cement.

### 3.3. Early Hydration Heat Evolution of Portland Cement Paste

The hydration exothermic rates and accumulative hydration heats of Portland cement paste for the control, Al1.0%, Na1.5%, and Al1.0% + Na1.5% groups are shown in Figure 3a,b. The early hydration of Portland cement was divided into five main periods, as shown in Figure 3a,b for I, II, III, IV and V, which indicated the initial reaction period (0–0.8 h), the induction period (0.8–3.6 h), the acceleration period (3.6–12.5 h), the deceleration period (12.5–30 h), and the stabilization period (>30 h), respectively [21,33,34].

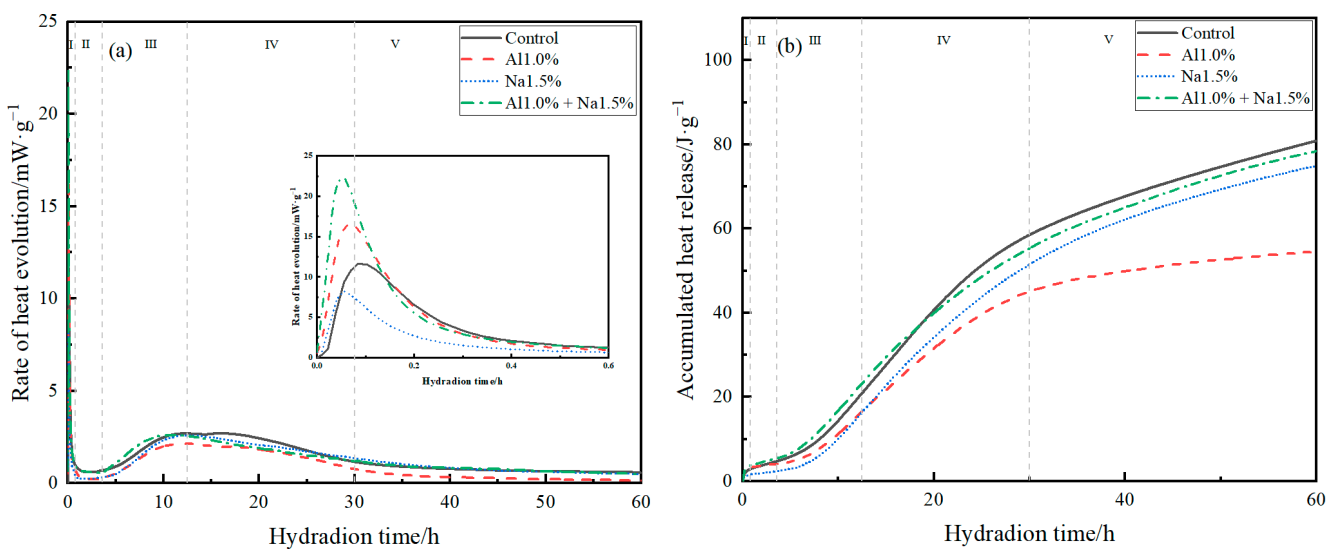


Figure 3. (a) hydration exothermic rates and (b) accumulative hydration heats of Portland cement paste.

As shown in Figure 3a, during the induction period, compared to the control group, the Al1.0% group accelerated hydration and increased the maximum rate of hydration during the induction period, while the Na1.5% group also promoted hydration at the beginning

of the induction period and brought the peak earlier, but reduced the maximum rate of hydration during the induction period. The Al1.0% + Na1.5% group greatly facilitated the hydration of the cement during the induction period, with the highest hydration rate during the induction period being approximately twice that of the control group. According to previous studies, the hydration of C<sub>3</sub>A to produce AFt and the reaction of aluminum sulfate and calcium hydroxide to produce AFt mainly take place during the induction period [35], therefore, it is believed that the Al1.0% + Na1.5% group greatly promoted the hydration of the cement during the induction period, with a large amount of AFt being produced. The hydration of C<sub>3</sub>S occurred mainly during the acceleration, deceleration, and stabilization periods [21]. It was observed that the Al1.0% + Na1.5% group caused the maximum hydration rate to occur earlier, thus promoting the hydration of C<sub>3</sub>S during the acceleration period and that there was also a very weak promotion of C<sub>3</sub>S hydration after 30 h.

According to Figure 3b, the cumulative hydration exotherm of the Al1.0% + Na1.5% group was higher than the other groups until about 20 h, and the cumulative hydration exotherm was smaller than that of the control group after 20 h hours. According to previous studies, the main factor affecting the rate of hydration of cement during the deceleration and stabilization phases is the diffusion rate [23], so the main reason for this phenomenon in the Al1.0% + Na1.5% group may be that the cement had formed a denser structure at this point compared to control, weakening the diffusion rate.

### 3.4. Hydration Products Analysis

#### 3.4.1. XRD Analysis

As shown in Figure 4, XRD analysis of specimens at 3 d and 28 d for the Al1.0%, Na1.5% and Al1.0% + Na1.5% groups revealed that the main hydration products of Portland cement paste contained AFt, AFm (monosulfate), Ca (OH)<sub>2</sub>, C–S–H, and un-hydrated products, such as C<sub>3</sub>S, C<sub>2</sub>S, C<sub>4</sub>AF, and CaCO<sub>3</sub> that had been carbonated.

As shown in Figure 4a,b, with 3 d of hydration, the height of the AFt diffraction peak in the Al1.0% + Na1.5% group was slightly higher than the Al1.0% group, and much higher than the Na1.5% group and control group, indicating that the Al1.0% + Na1.5% group promoted the production of more AFt. Furthermore, looking at the calcium hydroxide diffraction peaks ( $2\theta \approx 18^\circ$ ), it is clear that their peak heights were in descending order for the Al1.0% + Na1.5% group, the Na1.5% group, the Al1.0% group and the control group. This indicates that the Al1.0% + Na1.5% group at 3d had the least amount of calcium hydroxide, which corresponds to the production of more AFt consuming more calcium ions. Although the control group had the lowest calcium hydroxide diffraction peak ( $2\theta \approx 35^\circ$ ) compared to the other groups, it had the strongest and highest calcium carbonate diffraction peak, probably due to the lower density of the control group, which absorbed more carbon dioxide and produced more calcium carbonate. The generated AFt is cross-linked to form the early skeleton in the hydration of Portland cement paste, which is filled with generated C–S–H, CaCO<sub>3</sub>, etc. Then the generation of more AFt leads to a denser microstructure, which exhibits higher strength, and which confirms why the Al1.0% + Na1.5% group has a higher 3 d early strength.

According to Figure 4c,d, with 28 d of hydration, the AFt diffraction peaks of the Al1.0% + Na1.5% group are not very different from those of the Al1.0%, Na1.5% and control groups, but the AFm diffraction peaks are more pronounced than those of the other groups, which indicates that some of the AFt generated in the Al1.0% + Na1.5% group was converted to AFm. Comparing the diffraction peaks of calcium hydroxide ( $2\theta \approx 18^\circ$ ,  $2\theta \approx 35^\circ$ ) it is clear that the peak height of the Al1.0% + Na1.5% group was weaker while observing that the diffraction peaks of C<sub>3</sub>S and C<sub>2</sub>S were smaller for the Al1.0% + Na1.5% group than for the other three groups, which indicates that the synergistic use of 1.0% aluminum sulfate and 1.5% sodium sulfate promotes the hydration of Portland cement paste to a greater extent.

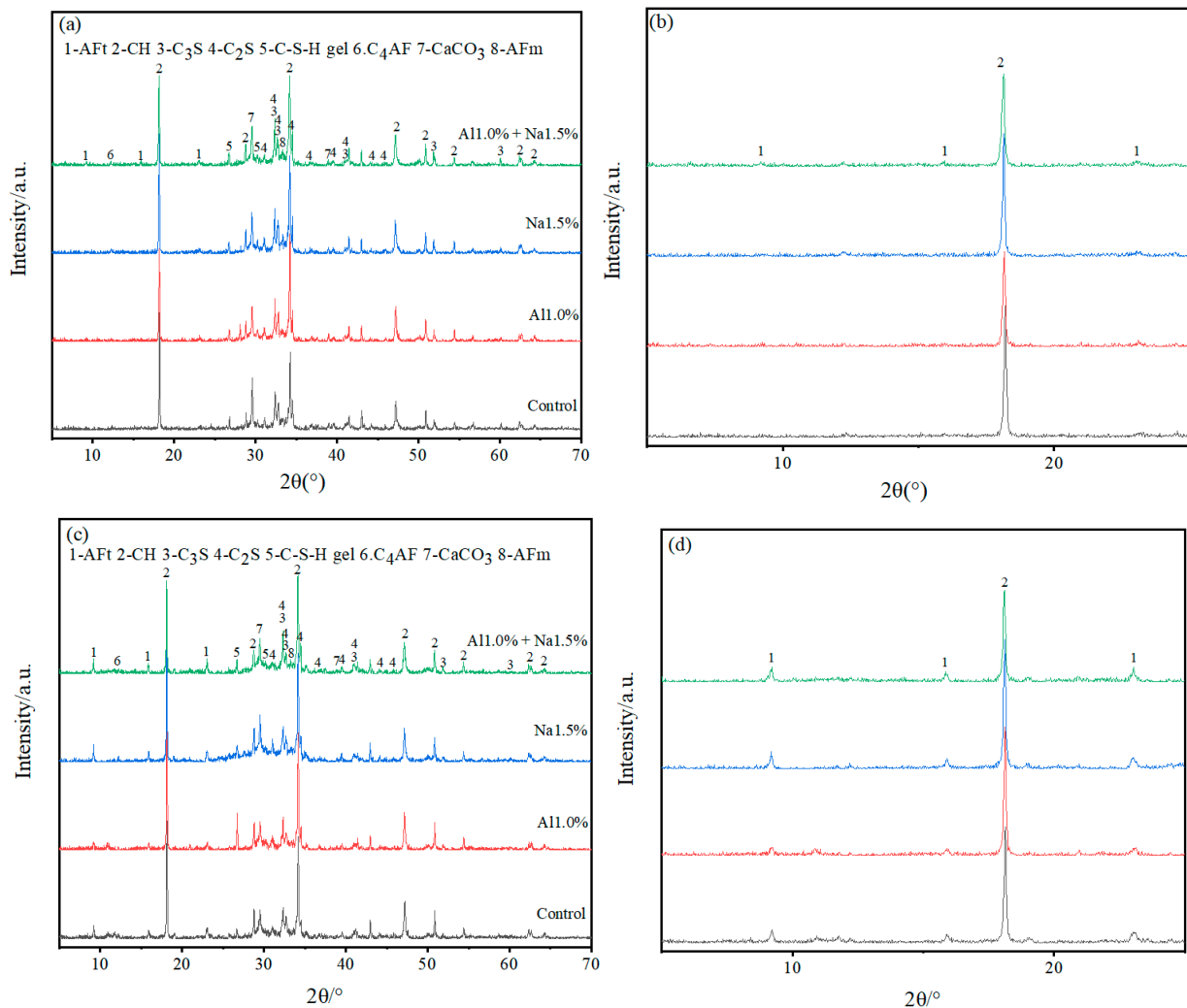


**Figure 4.** (a–d) are full-scale and locally magnified XRD patterns of Portland cement paste at 3 d and 28 d, respectively. (a) is full-scale XRD of Portland paste at 3 d, (b) is locally magnified XRD of Portland paste at 3 d, (c) is full-scale XRD of Portland paste at 28 d and (d) is locally magnified XRD of Portland paste at 28 d.

### 3.4.2. TG-DTG Analysis

To further analyze the hydration products composition of Portland cement paste, Figure 5a,b shows the TG-DTG curves of Portland cement paste at 3 d and 28 d. In the thermogravimetric analysis diagram of Portland cement paste, there are three main stages of heat absorption peaks, the first of which is subdivided into two subsections, heat loss from loss of bound water at 80–150 °C for AFt, heat loss from loss of bound water at 150–200 °C for AFm, heat loss from thermal decomposition of  $\text{Ca}(\text{OH})_2$  to CaO and water vapor at 370–480 °C, and heat loss from thermal decomposition of  $\text{CaCO}_3$  to CaO and  $\text{CO}_2$  at 490–800 °C [36–38].

According to Figure 5, the amount of AFt and CH produced can be calculated and shown in Table 5. Figure 5a and Table 5 shows that the amount of AFt generated in the All.0% group was more significant than that in the control group. While observing the DTG curves, it can be found that the All.0% group had a larger peak at 150–200 °C and produced less CH than the control group, which indicates that the 1.0% of aluminum sulfate consumed some of the calcium ions and promoted the production of AFt, the reduction of CH and the hydration of  $\text{C}_3\text{S}$ , which in turn led to an increase in the early strength of Portland cement paste, as also proved by Liu et al. [3,21]. The AFt produced in the Na1.5% group was not significantly different compared to the control group, but the

peak at 150–200 °C was slightly larger in the Na1.5% group than that in the control group, and the amount of CH produced in the Na1.5% group was much lower than in the control group, indicating that 1.0% of sodium sulfate promoted the hydration of  $C_3A$  and  $C_3S$  and improved the early strength of Portland cement paste, which is consistent with the studies of Mei et al. [23,33,39]. The Al1.0% + Na1.5% group had the highest AFt production. At the same time, a larger peak at 150–200 °C was observed in the DTG curve, which was due to a lower ratio of calcium sulfate to aluminates to promote conversion from more AFt into AFm [40–42]. Additionally, there was a lower mass of CH production, which demonstrates that 1.0% of aluminum sulfate and 1.5% of sodium sulfate were synergistic, promoting more AFt generation, and better hydration of  $C_3A$  and  $C_3S$ , resulting in a tighter early structure and higher early strength at 3 d.

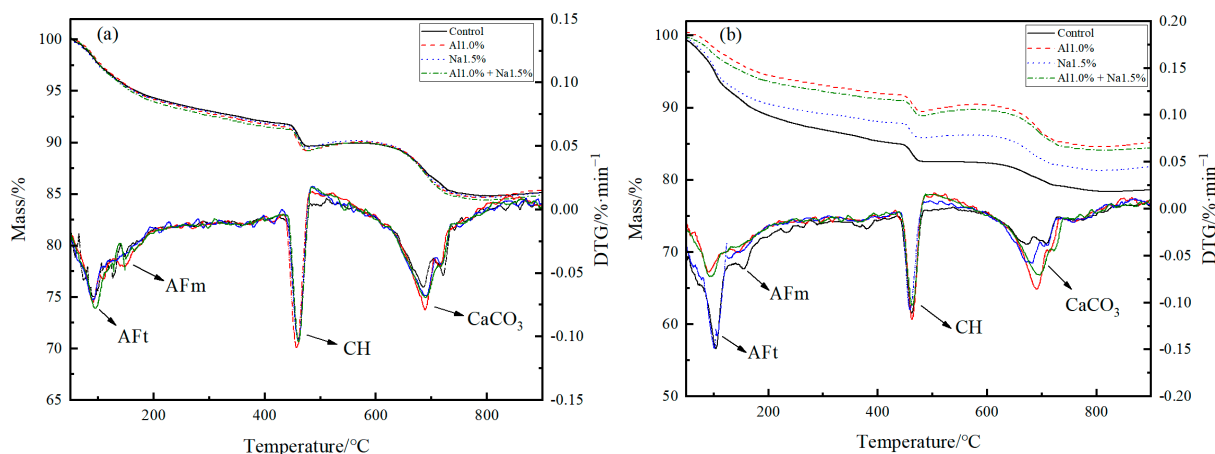


**Figure 5.** TG-DTG curves of Portland cement paste at (a) 3 d and (b) 28 d with different admixture.

**Table 5.** The amount of AFt and CH produced at 3 d by calculating the mass loss of Portland cement paste.

No.	$m_{AFt}/\%$	$m_{CH}/\%$	$m_{CC}/\%$	$m_{CH}/\%$
Control	10.27	2.37	4.85	16.28
Al1.0%	10.81	2.02	4.86	15.53
Na1.5%	10.21	2.02	5.14	16.17
Al1.0% + Na1.5%	11.33	1.84	5.18	15.85

Figure 5b and Table 6 show that the CH production of the Al1.0% group was almost the same as that of the control, which indicated that 1.0% of aluminum sulfate promoted the hydration of  $C_3S$ . Brykov et al. [43] attributed the promotion of  $C_3S$  hydration by aluminum sulfate at a later stage to the compressive effect of  $Al^{3+}$  on the C–S–H layer, which promotes C–S–H aggregation. Higher CH production in the later stages caused more CH to be carbonated. He et al. also demonstrated that the  $CaCO_3$  generated by carbonation filling the Portland cement paste pores could stabilize the Portland cement paste [44–46]. The Na1.5% group generated less CH than the control group. The phenomenon that the 1.5% of sodium sulfate promoted the hydration of  $C_3S$ , as shown by the heat of hydration and XRD analysis, as well as the increased compressive strength of the 28 d Na1.5% group, is thought to be the result of the addition of 1.5% of sodium sulfate promoting the generation of sodium hydroxide. The reduction of CH, along with the generation of sodium hydroxide enhances the solubility of  $C_3S$ ,  $C_2S$ , which together promote the hydration of  $C_3S$ ,  $C_2S$  [2,13,47]. According to Le Chatelier’s principle [48,49], the CH production in the Al1.0% + Na1.5% group was less than the control and Al1.0% groups, but more than the Na1.5% group, so 1.0% of aluminum sulfate and 1.5% of sodium sulfate synergistically promote the hydration of late cement. Ratios of 1.0% of aluminum sulfate and 1.5% of sodium sulfate synergistically contribute more to the hydration of  $C_3S$  and  $C_2S$  in the later stages of Portland cement paste. Wang et al. [50] concluded that the development of late

strength in cement was mainly related to the C–S–H generated by the hydration of  $C_3S$  and  $C_2S$  in cement. More C–S–H filling in the Portland cement paste aggregate leads to a denser structure and higher strength, which confirms that 1.0% of aluminum sulfate and 1.5% of sodium sulfate synergistically promote the hydration of  $C_3S$  and  $C_2S$ , with the best compressive strength performance at 28 d.

**Table 6.** The amount of AFt and CH produced at 28 d by calculating the mass loss of Portland cement paste.

No.	$m_{AFt}/\%$	$m_H/\%$	$m_{CC}/\%$	$m_{CH}/\%$
Control	18.96	3.33	3.89	16.24
Al1.0%	10.93	1.90	5.32	16.30
Na1.5%	17.45	2.22	4.44	15.02
Al1.0% + Na1.5%	11.15	1.75	5.31	15.95

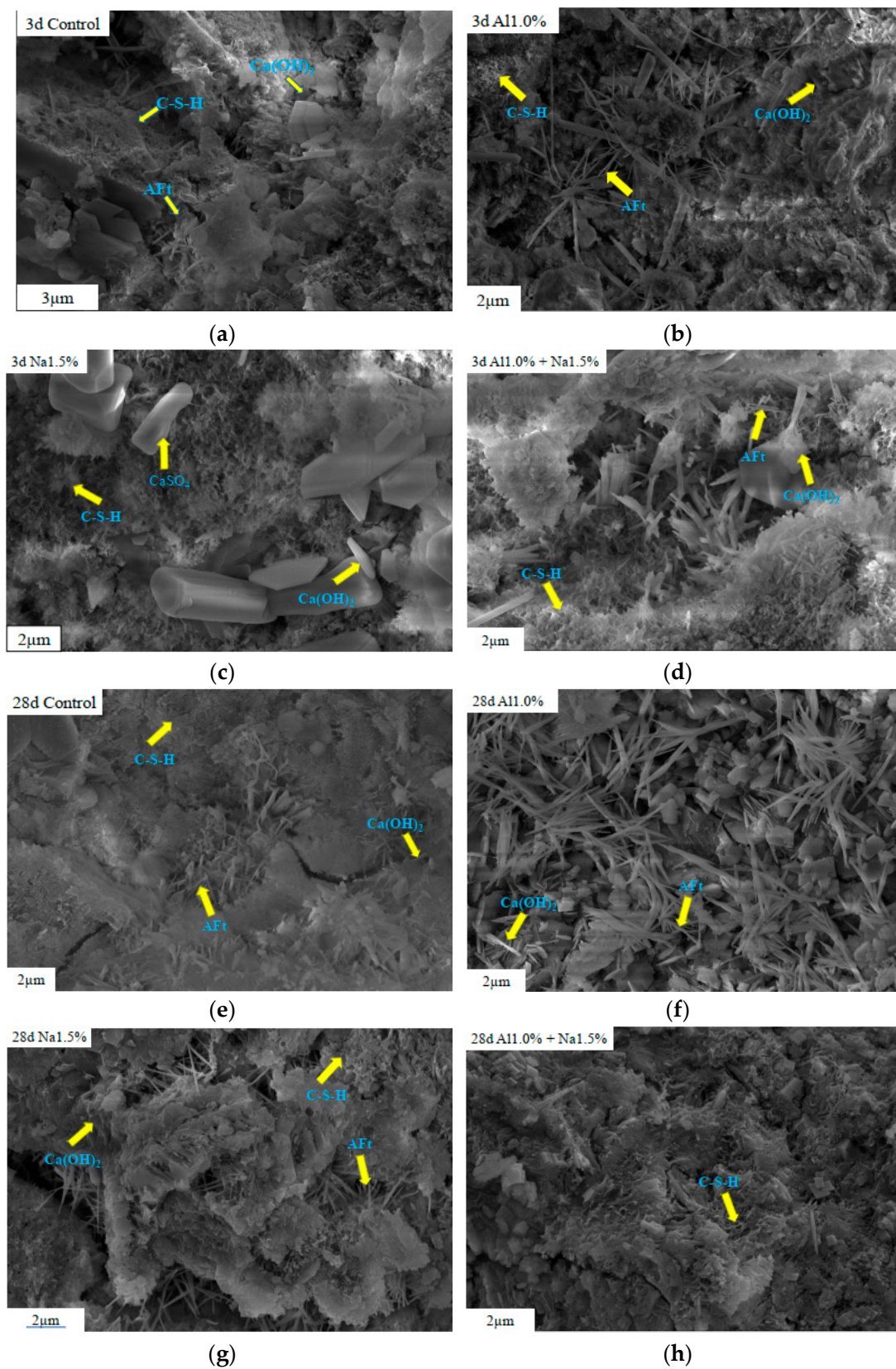
### 3.5. Microstructure Observation

The SEM images (Figure 6a–h) of the 3 d Na1.5% group showed that a large amount of C–S–H was generated and covered the cement particles. At the same time, some CH and  $CaCO_3$  were also filled in the cement skeleton, resulting in denser microstructure and better compressive strength than the control group at 3 d. As for the 3 d Al1.0% group, it clearly shows a large amount of AFt being densely interacted together, which makes the cement paste denser than the 3-d control group and has higher compressive strength. Observing the SEM of the Al1.0% + Na1.5% group reveals that there is dense AFt being intercalated, the amount of AFt is denser than that of the Al1.0% group and much denser than that of the control group. Moreover, it can see that more C–S–H was generated to be filled in compared to the other groups, which resulted in a denser structure and showed the desired early strength. These are consistent with the results of XRD and TG-DTG analyses that more AFt can be formed and the hydration of  $C_3S$  was also accelerated to make the Portland cement paste more compact.

Observation of the scanning electron microscopy pattern clearly shows that the Portland cement paste at 28 d was more fully hydrated than the Portland cement paste at 3 d. Although the Na1.5% group at 28 d also appears to have a dense structure, the structure is accompanied by large cracks, which affect the compressive strength of Portland cement paste. Cracking in the cement of the Na1.5% group at 28 d is thought to be initiated by water loss and re-crystallization of soluble sodium salts [13,28,51,52]. According to the observation of the mapping of the Al1.0% group at 28 d, it shows that the structure of this group was denser than that of the 28-d control group. According to the observation of the SEM pattern of the 28 d Al1.0% + Na1.5% group, it can be found that a large amount of C–S–H is filled in the cement paste. There were almost no large cracks on the surface of the 28 d Al1.0% + Na1.5% group compared to the 28-d control group, the 28 d Al1.0% group and the 28 d Na1.5% group. At the same time, there were some small particles embedded in the C–S–H, which would explain that structure of the 28 d Al1.0% + Na1.5% group was the densest; this phenomenon is better demonstrated in the chapter on the pore structure.

### 3.6. Pore Structure Evolution

The properties of an already hardened cement paste are related to the pore structure in addition to the already hydrated products and the anhydrate particles. The characterization of the pore structure involves porosity, pore size distribution, and pore size. The pore size in cementitious composites are classified into four categories according to the hazard posed by the size of the pores: no harmful pore size (<20 nm), less harmful pores (20–50 nm), harmful pores (50–200 nm), and more harmful pores (>200 nm) [53,54]. Relevant MIP test data are summarized in Table 7.

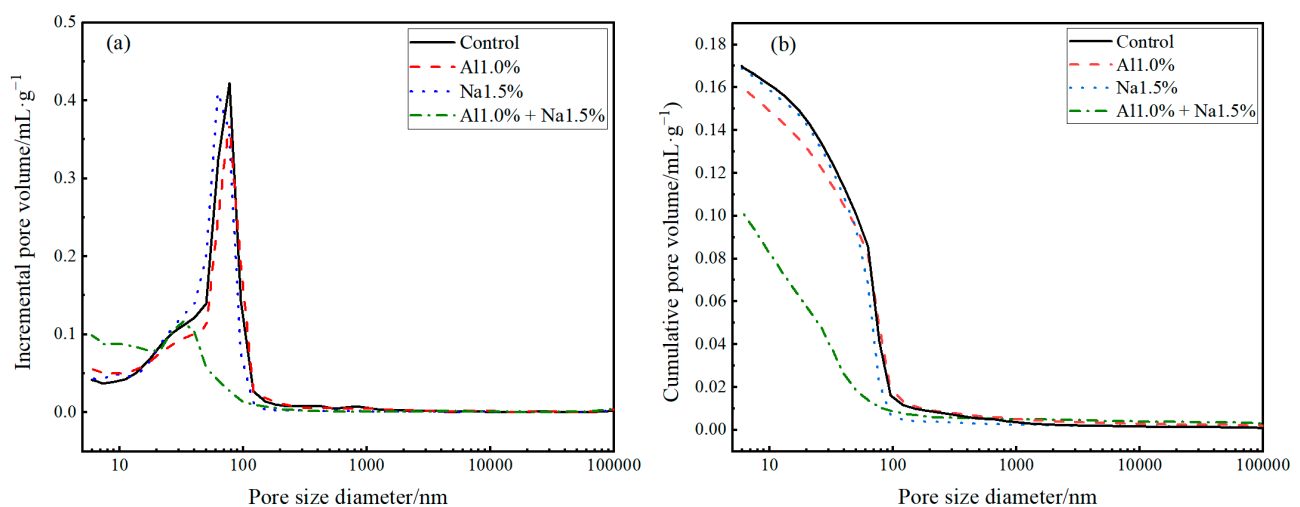


**Figure 6.** SEM images of Portland cement paste at 3 d and 28 d with different admixture. (a) is SEM images of Control at 3 d (b) is SEM images of Al1.0% at 3 d, (c) is SEM images of Na1.5% at 3 d, (d) is SEM images of Al1.0% + Na1.5% at 3 d, (e) is SEM images of Control at 28 d, (f) is SEM images of Al1.0% at 28 d, (g) is SEM images of Na1.5% at 28 d and (h) is SEM images of Al1.0% + Na1.5% at 28 d.

**Table 7.** Porosity and pore size distribution of paste with different admixture.

Groups	Average Pore Size ( $\mu\text{m}$ )	Porosity (%)	Proportion of Pore Size (%)			
			$\leq 20$ nm	20~50 nm	50~200 nm	$\geq 200$ nm
Control	0.03444	50.1	16.0	24.7	54.5	3.1
Al1.0%	0.03183	61.4	19.0	22.1	53.4	5.5
Na1.5%	0.03198	48.2	16.8	27.8	53.3	2.3
Al1.0% + Na1.5%	0.01736	36.1	45.7	36.3	11.9	5.8

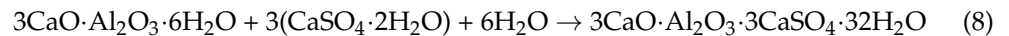
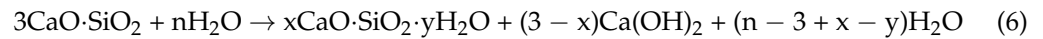
According to Table 7, the Al1.0% + Na1.5%, Al1.0% and Na1.5% groups all reduced the average pore size of Portland cement paste compared to the control group, but the Al1.0% + Na1.5% group was the more effective. The average pore size for the Al1.0% + Na1.5% group was 0.01736  $\mu\text{m}$ , a reduction of 49.6% compared to the control group, while the Al1.0% and Na1.5% groups showed a decrease of 7.5% and 7.0%, respectively. Furthermore, according to Table 7, the Portland cement paste porosity was reduced in the Al1.0% + Na1.5% and Na1.5% groups compared to the control group. The total porosity of the Al1.0% + Na1.5% group was the smallest, with a 27.9% reduction compared to the control group. Initially, regarding the Al1.0% + Na1.5% group, no harm and less harmful pores accounted for 45.7% and 36.6% of the total porosity, respectively, while no harm and less harmful pores in the Na1.5% group accounted for 16.8% and 27.8% of the total porosity, respectively. Regarding the Al1.0% group, although the total porosity was higher than that of the control group, no harm and less harmful pores accounted for 19.0% and 22.1% of the total porosity, respectively, which was a higher percentage than the control group. Meanwhile according to Figure 7a,b, 1.0% aluminum sulfate and 1.5% of sodium sulfate affected the porosity and pore size distribution of Portland cement paste in varying degrees, which increases the compressive strength of Portland cement paste. The simultaneous use of 1.0% aluminum sulfate and 1.5% of sodium sulfate has a synergistic effect on the denseness of Portland cement paste, not only reducing the porosity but also decreasing the proportion of harmful and porous pores, which is one of the main reasons for the higher compressive strength at 28 d of the Al1.0% + Na1.5% group [55].

**Figure 7.** Effect of the different admixture Portland content on the pore structure of the hardened cement paste, (a) pore size distribution, (b) cumulative pore volume.

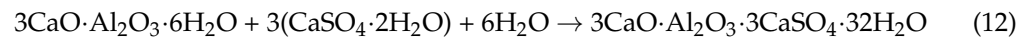
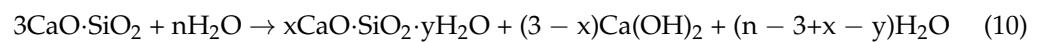
### 3.7. Discussion

Combined with previous studies and the macroscopic and microscopic test analysis of this experiment, we can infer that aluminum sulfate can promote the formation of AFt from

C<sub>3</sub>A in cement paste, and the introduced Al<sup>3+</sup> can react with Ca<sup>2+</sup>, (OH)<sup>−</sup>, SO<sub>4</sub><sup>2−</sup> and water to form AFt. A large amount of AFt produced will crosslink to form the early skeleton of Portland cement paste. Compared to the control group, the considerable reduction of Ca<sup>2+</sup> and (OH)<sup>−</sup> will rapidly promote the hydration of C<sub>3</sub>S, then be weakened by the rapid decrease in C<sub>3</sub>S, when again promote the hydration of C<sub>3</sub>S and C<sub>2</sub>S at after 48 h due to the compression of the C–S–H layer by Al<sup>3+</sup> [3,20,21,43].



The addition of sodium sulfate to cement produces CaSO<sub>4</sub>·2H<sub>2</sub>O, which promotes the hydration of C<sub>3</sub>A to form AFt, the free Na<sup>+</sup> will combine with OH<sup>−</sup> to form NaOH, which will increase the solubility of Ca<sup>2+</sup> and promote the hydration of C<sub>3</sub>S to form C–S–H [23,27,33]. However, soluble sodium salts in silicate cement paste will lose water and recrystallize in the later stage, which leads to swelling and cracking of Portland cement paste and affects its strength [28,51].



when aluminum sulfate and sodium sulfate are used synergistically, the introduced SO<sub>4</sub><sup>2−</sup>, Al<sup>3+</sup> and Na<sup>+</sup> work together to promote the generation of more AFt. The rapid reduction of Ca<sup>2+</sup> and (OH)<sup>−</sup> in the Portland cement paste, the increased solubility of C<sub>3</sub>S and C<sub>2</sub>S by the generated NaOH, and the fast aggregation of C–S–H layers by the compression of Al<sup>3+</sup>, all work together to promote the hydration of C<sub>3</sub>S and C<sub>2</sub>S in the Portland cement paste. According to Section 2.2.9, the Al1.0% + Na1.5% group had a smaller average pore size, and fewer harmful pores. The reason for this phenomenon is that more AFt cross-linking occurring early on makes the cement paste denser, and more hydration products such as C–S–H fill it. At the same time, Al<sup>3+</sup> ions compress C–S–H, which reduces the porosity of the cement paste, reduces the average pore size, and makes the cement paste more compact, showing higher early compressive strength. Then, in the later stages there is still hydration of C<sub>2</sub>S, which produces a continuous squeeze of C–S–H and makes the cement paste more compact.

#### 4. Conclusions

In this work, different doses of aluminum sulfate and sodium sulfate, and the synergistic use of different doses of the DSAs as early strengthening agents were used to improve the performance of Portland cement paste. The setting and hardening properties of Portland cement paste were investigated with different admixtures and dosing ratios, the microstructure and hydration product composition of products were also analyzed separately. Finally, the mechanism of action when used singly and in combination was discussed. The results and discussion are summarized as follows.

- (1) The early compressive strength of Portland cement paste at 3 d was significantly increased when using 1.0% of aluminum sulfate and 1.5% of sodium sulfate in combination, and the compressive strength at 28 d was also the best. The compressive strength at 3 d and 28 d were 40.4 MPa and 64.2 MPa, respectively, increasing 21.3% and 29.7% over the control group, 13.2% and 5.9% over the Al1.0% group, and 10.1% and 7.5% over Na1.5%, respectively.

- (2) Compared to the control group, the use of aluminum sulfate promoted the hydration of  $C_3A$ , the reaction of  $Al^{3+}$ ,  $Ca^{2+}$ , and  $(OH)^-$  ions promoted the production of more AFt, while the reduction of  $Ca^{2+}$  and  $(OH)^-$  ions rapidly promoted the hydration of  $C_3S$ . The addition of sodium sulfate promoted the generation of a certain amount of  $CaSO_4 \cdot H_2O$ , thus facilitating the hydration of  $C_3A$  to produce AFt, and the presence of  $Na^+$  and  $(OH)^-$  ions combined to promote the solubility of  $C_3S$  in the paste. When aluminum sulfate and sodium sulfate were used together, they synergistically promoted the hydration of  $C_3A$  to produce AFt, facilitating the production of more AFt and the hydration of  $C_3S$  and  $C_2S$  to produce more C–S–H.
- (3) The synergistic use of 1.0% of aluminum sulfate and 1.5% of sodium sulfate resulted in the generation of more AFt in the Portland cement paste, which was cross-linked together to form the early skeleton of Portland cement paste base, and the products generated such as C–S–H,  $CaCO_3$  and  $CaSO_4 \cdot H_2O$  were filled in. Compared to the control group, the Al1.0% group, and the Na1.5% group, the Al1.0% + Na1.5% group resulted in a denser structure with reduced porosity, fewer harmful pores and more harmless pores, which allowed the Portland cement paste to exhibit a higher compressive strength.

**Author Contributions:** Conceptualization, L.S.; data curation, L.S.; formal analysis, Y.W.; funding acquisition, Y.W. and S.L. (Songhui Liu); investigation, L.S. and S.L. (Shuaijie Li); methodology, Y.W., S.L. (Songhui Liu), S.L. (Shuqiong Luo) and X.G.; project administration, Y.W.; resources, Y.W., S.L. (Songhui Liu), X.G. and S.L. (Shuqiong Luo); supervision, Y.W. and S.L. (Songhui Liu); validation, L.S. and S.L. (Shuaijie Li); writing—original draft, L.S.; writing—review and editing, Y.W., L.S., S.L. (Songhui Liu), X.G. and S.L. (Shuqiong Luo). All authors have read and agreed to the published version of the manuscript.

**Funding:** This work was supported by the National Natural Science Foundation of China (52108208), the fellowship of China Postdoctoral Science Foundation (2020M682290), the science and technology project of Henan Province (211110231400, 212102310559), the National Key R&D Program Intergovernmental International Science and Technology Innovation Cooperation Project (2018YFE0107300), the Opening Project of State Key Laboratory of Green Building Materials (2021GBM06), the Henan Outstanding Foreign Scientists' Workroom (GZS2021003), the doctor foundation of Henan Polytechnic University (B2020-11), and the Fundamental Research Funds for the Universities of Henan Province (NSFRF220302).

**Institutional Review Board Statement:** Not applicable.

**Informed Consent Statement:** Not applicable.

**Data Availability Statement:** Not applicable.

**Conflicts of Interest:** The authors declare no conflict of interest.

## References

1. Aggoun, S.; Cheikh-Zouaoui, M.; Chikh, N.; Duval, R. Effect of some admixtures on the setting time and strength evolution of cement pastes at early ages. *Constr. Build. Mater.* **2008**, *22*, 106–110. [[CrossRef](#)]
2. Wu, M.; Zhang, Y.; Jia, Y.; She, W.; Liu, G.; Yang, Z.; Zhang, Y.; Zhang, W.; Sun, W. Effects of sodium sulfate on the hydration and properties of lime-based low carbon cementitious materials. *J. Clean. Prod.* **2019**, *220*, 677–687. [[CrossRef](#)]
3. Liu, S.; Shen, Y.; Wang, Y.; He, H.; Luo, S.; Huang, C. Synergistic use of sodium bicarbonate and aluminum sulfate to enhance the hydration and hardening properties of Portland cement paste. *Constr. Build. Mater.* **2021**, *299*, 124248. [[CrossRef](#)]
4. Heren, Z.; Ölmez, H. The influence of ethanolamines on the hydration and mechanical properties of Portland cement. *Cem. Concr. Res.* **1996**, *26*, 701–705. [[CrossRef](#)]
5. Bao, J.; Ren, Q.; Sun, L.; Ding, Y.; Oh, W.-C. Preparation of an Early Strengthening Agent for Concrete under Low-Temperature Conditions and Evaluation of Its Reaction Mechanism. *Korean J. Mater. Res.* **2021**, *31*, 195–208. [[CrossRef](#)]
6. Lee, T.; Lee, J.; Choi, H.; Lee, D. The Effects of Fineness and TEA-Based Chemical Admixture on Early Strength Development of Concrete in Construction Site Applications. *Materials* **2020**, *13*, 2027. [[CrossRef](#)]
7. Izotov, V.S.; Ibragimov, R.A. Hydration Products of Portland Cement Modified with a Complex Admixture. *Inorg. Mater.* **2015**, *2*, 87–190. [[CrossRef](#)]

8. Izotov, V.S.; Ibragimov, R.A. Influence of additives-hardening accelerators on the properties of heavy concrete. *Stroit. Mater.* **2010**, *3*, 35–37.
9. Fakhri, M.; Yousefian, F.; Amoosoltani, E.; Aliha, M.R.M.; Berto, F. Combined effects of recycled crumb rubber and silica fume on mechanical properties and mode I fracture toughness of self-compacting concrete. *Fatigue Fract. Eng. Mater. Struct.* **2021**, *44*, 2659–2673. [[CrossRef](#)]
10. Fakhri, M.; Amoosoltani, E. Crack behavior analysis of roller compacted concrete mixtures containing reclaimed asphalt pavement and crumb rubber. *Eng. Fract. Mech.* **2017**, *180*, 43–59. [[CrossRef](#)]
11. Fakhri, M.; Amoosoltani, E. The effect of Reclaimed Asphalt Pavement and crumb rubber on mechanical properties of Roller Compacted Concrete Pavement. *Constr. Build. Mater.* **2017**, *137*, 470–484. [[CrossRef](#)]
12. Fakhri, M.; Saberi, K.F. The effect of waste rubber particles and silica fume on the mechanical properties of Roller Compacted Concrete Pavement. *J. Clean. Prod.* **2016**, *129*, 521–530. [[CrossRef](#)]
13. Jiang, M.; Lv, X. Progress in Research and Application of early strength of concrete. *Bull. Chin. Silic. Soc.* **2014**, *33*, 2527–2533.
14. Chen, S.; Du, Z.; Zhang, Z.; Zhang, H.; Xia, Z.; Feng, F. Effects of chloride on the early mechanical properties and microstructure of gangue-cemented paste backfill. *Constr. Build. Mater.* **2020**, *235*, 117504. [[CrossRef](#)]
15. Wang, J.; Qian, C.; Qu, J.; Guo, J. Effect of lithium salt and nano nucleating agent on early hydration of cement based materials. *Constr. Build. Mater.* **2018**, *174*, 24–29. [[CrossRef](#)]
16. Lu, C.; Yuan, S.; Cheng, P.; Liu, R. Mechanical properties of corroded steel bars in pre-cracked concrete suffering from chloride attack. *Constr. Build. Mater.* **2016**, *123*, 649–660. [[CrossRef](#)]
17. Ren, G.; Tian, Z.; Wu, J.; Gao, X. Effects of combined accelerating admixtures on mechanical strength and microstructure of cement mortar. *Constr. Build. Mater.* **2021**, *304*, 124642. [[CrossRef](#)]
18. Paglia, C.; Wombacher, F.; Böhni, H. The influence of alkali-free and alkaline shotcrete accelerators within cement systems: I. Characterization of the setting behavior. *Cem. Concr. Res.* **2001**, *31*, 913–918. [[CrossRef](#)]
19. Prudêncio, L.R. Accelerating admixtures for shotcrete. *Cem. Concr. Compos.* **1998**, *20*, 213–219. [[CrossRef](#)]
20. Yang, R.; He, T.; Guan, M.; Guo, X.; Xu, Y.; Xu, R.; Da, Y. Preparation and accelerating mechanism of aluminum sulfate-based alkali-free accelerating additive for sprayed concrete. *Constr. Build. Mater.* **2020**, *234*, 117334. [[CrossRef](#)]
21. Liu, X.; Ma, B.; Tan, H.; Gu, B.; Zhang, T.; Chen, P.; Li, H.; Mei, J. Effect of aluminum sulfate on the hydration of Portland cement, tricalcium silicate and tricalcium aluminate. *Constr. Build. Mater.* **2020**, *232*, 117179. [[CrossRef](#)]
22. Chen, C.; Sun, Z. Influence of Aluminum Sulfate on Hydration and Properties of Cement Pastes. *J. Adv. Concr. Technol.* **2018**, *16*, 522–530. [[CrossRef](#)]
23. Li, H.; Xue, Z.; Liang, G.; Wu, K.; Dong, B.; Wang, W. Effect of C–S–H s-PCE and sodium sulfate on the hydration kinetics and mechanical properties of cement paste. *Constr. Build. Mater.* **2021**, *266*, 121096. [[CrossRef](#)]
24. Zou, F.; Hu, C.; Wang, F.; Ruan, Y.; Hu, S. Enhancement of early-age strength of the high content fly ash blended cement paste by sodium sulfate and C–S–H seeds towards a greener binder. *J. Clean. Prod.* **2020**, *244*, 118566. [[CrossRef](#)]
25. Fu, J.; Jones, A.M.; Bligh, M.W.; Holt, C.; Keyte, L.M.; Moghaddam, F.; Foster, S.J.; Waite, T.D. Mechanisms of enhancement in early hydration by sodium sulfate in a slag-cement blend—Insights from pore solution chemistry. *Cem. Concr. Res.* **2020**, *135*, 106110. [[CrossRef](#)]
26. Zhao, Y.; Bai, H. Effect of early-strength admixture for concrete performance. *LiaoNing Build. Mater.* **2009**, *7*, 19–21.
27. Tan, H.; Deng, X.; He, X.; Zhang, J.; Zhang, X.; Su, Y.; Yang, J. Compressive strength and hydration process of wet-grinded granulated blast-furnace slag activated by sodium sulfate and sodium carbonate. *Cem. Concr. Compos.* **2019**, *97*, 387–398. [[CrossRef](#)]
28. Campos, A.; López, C.M.; Blanco, A.; Aguado, A. Effects of an internal sulfate attack and an alkali-aggregate reaction in a concrete dam. *Constr. Build. Mater.* **2018**, *166*, 668–683. [[CrossRef](#)]
29. GB175-2007; Common Portland Cement. Standardization Administration of China: Beijing, China, 2017.
30. GB/T 1346-2011; Test Methods for Water Requirement of Normal Consistency, Setting Time and Soundness of the Portland Cement. Standardization Administration of China: Beijing, China, 2011.
31. GB/T 50081-2019; Standard for Test Method of Concrete Physical and Mechanical Properties. Standardization Administration of China: Beijing, China, 2019.
32. Ma, B.; Zhang, T.; Tan, H.; Liu, X.; Mei, J.; Qi, H.; Jiang, W.; Zou, F. Effect of triisopropanolamine on compressive strength and hydration of cement-fly ash paste. *Constr. Build. Mater.* **2018**, *179*, 89–99. [[CrossRef](#)]
33. Mei, J.; Tan, H.; Li, H.; Ma, B.; Liu, X.; Jiang, W.; Zhang, T.; Li, X. Effect of sodium sulfate and nano-SiO<sub>2</sub> on hydration and microstructure of cementitious materials containing high volume fly ash under steam curing. *Constr. Build. Mater.* **2018**, *163*, 812–825. [[CrossRef](#)]
34. Dai, J.; Wang, Q.; Lou, X.; Bao, X.; Zhang, B.; Wang, J.; Zhang, X. Solution calorimetry to assess effects of water-cement ratio and low temperature on hydration heat of cement. *Constr. Build. Mater.* **2021**, *269*, 121222. [[CrossRef](#)]
35. Zhang, J.; Li, G.; Ye, W.; Chang, Y.; Liu, Q.; Song, Z. Effects of ordinary Portland cement on the early properties and hydration of calcium sulfoaluminate cement. *Constr. Build. Mater.* **2018**, *186*, 1144–1153. [[CrossRef](#)]
36. Luo, S.Q.; Zhao, M.H.; Jiang, Z.Z.; Liu, S.H.; Yang, L.; Mao, Y.X.; Pan, C.G. Microwave preparation and carbonation properties of low-carbon cement. *Constr. Build. Mater.* **2021**, *320*, 126239. [[CrossRef](#)]

37. Guan, X.; Liu, S.; Feng, C.; Qiu, M. The hardening behavior of  $\gamma$ -C2S binder using accelerated carbonation. *Constr. Build. Mater.* **2016**, *114*, 204–207. [[CrossRef](#)]
38. Jain, J.; Neithalath, N. Analysis of calcium leaching behavior of plain and modified cement pastes in pure water. *Cem. Concr. Compos.* **2009**, *31*, 176–185. [[CrossRef](#)]
39. Criado, M.; Jiménez, A.F.; Palomo, A. Effect of sodium sulfate on the alkali activation of fly ash. *Cem. Concr. Compos.* **2010**, *32*, 589–594. [[CrossRef](#)]
40. Andrade Neto, J.S.; de Matos, P.R.; De la Torre, A.G.; Campos, C.E.M.; Gleize, P.J.P.; Monteiro, P.J.M.; Kirchheim, A.P. The role of sodium and sulfate sources on the rheology and hydration of C3A polymorphs. *Cem. Concr. Res.* **2022**, *151*, 106639. [[CrossRef](#)]
41. Joseph, S.; Skibsted, J.; Cizer, Ö. A quantitative study of the C3A hydration. *Cem. Concr. Res.* **2019**, *115*, 145–159. [[CrossRef](#)]
42. Quennoz, A.; Scrivener, K.L. Hydration of C3A–gypsum systems. *Cem. Concr. Res.* **2012**, *42*, 1032–1041. [[CrossRef](#)]
43. Brykov, A.S.; Vasil Ev, A.S.; Mokeev, M.V. Hydration of portland cement in the presence of aluminum-containing setting accelerators. *Russ. J. Appl. Chem.* **2013**, *86*, 793–801. [[CrossRef](#)]
44. He, H.; Wang, Y.; Wang, J. Compactness and hardened properties of machine-made sand mortar with aggregate micro fines. *Constr. Build. Mater.* **2020**, *250*, 118828. [[CrossRef](#)]
45. Liu, S.; Zhang, H.; Wang, Y.; Gou, M. Carbon-dioxide-activated bonding material with low water demand. *Adv. Cem. Res.* **2021**, *33*, 193–196. [[CrossRef](#)]
46. Liu, S.; Shen, P.; Xuan, D.; Li, L.; Sojobi, A.; Zhan, B.; Poon, C.S. A comparison of liquid-solid and gas-solid accelerated carbonation for enhancement of recycled concrete aggregate. *Cem. Concr. Compos.* **2021**, *118*, 103988. [[CrossRef](#)]
47. Rashad, A.M.; Bai, Y.; Basheer, P.A.M.; Milestone, N.B.; Collier, N.C. Hydration and properties of sodium sulfate activated slag. *Cem. Concr. Compos.* **2013**, *37*, 20–29. [[CrossRef](#)]
48. Cai, J. The correct application of chemical equilibrium Le chatelier's principle to judge the direction of movement. *Fujian Basic Educ. Res.* **2013**, *11*, 40–41.
49. Lin, Y. Correctly Understanding and Using Le chatelier's principle. *Chem. Educ.* **2012**, *33*, 3.
50. Wang, L.; Yang, H.; Zhou, S.; Chen, E.; Tang, S. Hydration, mechanical property and C–S–H structure of early-strength low-heat cement-based materials. *Mater. Lett.* **2018**, *217*, 151–154. [[CrossRef](#)]
51. Comi, C.; Perego, U. Anisotropic Damage Model for Concrete Affected by Alkali-Aggregate Reaction. *Int. J. Damage Mech.* **2011**, *4*, 598–617. [[CrossRef](#)]
52. Owsiak, Z.; Zapała-Sławeta, J.; Czapik, P. Diagnosis of concrete structures distress due to alkali-aggregate reaction. *Bull. Pol. Acad. Sci. Tech. Sci.* **2015**, *63*, 23–29. [[CrossRef](#)]
53. Zhang, B.; Tan, H.; Ma, B.; Chen, F.; Lv, Z.; Li, X. Preparation and application of fine-grinded cement in cement-based material. *Constr. Build. Mater.* **2017**, *157*, 34–41. [[CrossRef](#)]
54. Pang, B.; Zhou, Z.; Xu, H. Utilization of carbonated and granulated steel slag aggregate in concrete. *Constr. Build. Mater.* **2015**, *84*, 454–467. [[CrossRef](#)]
55. Xue, J.; Liu, S.; Ma, X.; Teng, Y.; Guan, X. Effect of different gypsum dosage on the chloride binding properties of C4AF hydrated paste. *Constr. Build. Mater.* **2022**, *315*, 125562. [[CrossRef](#)]